

STORM: Slot-based Task-aware Object-centric Representation for robotic Manipulation

Alexandre Chapin^{1[0009-0000-3779-9387]}, Emmanuel Dellandrea^{1[0000-0001-7346-228X]}, and Liming Chen^{1[0000-0002-3654-9498]}

Ecole Centrale de Lyon `{first-name.surname}@ec-lyon.fr`

Abstract. Visual foundation models provide strong perceptual features for robotics, but their dense representations lack explicit object-level structure, limiting robustness and controllability in manipulation tasks. We propose STORM (Slot-based Task-aware Object-centric Representation for robotic Manipulation), a lightweight object-centric adaptation module that augments frozen visual foundation models with a small set of semantic-aware slots for robotic manipulation. Rather than retraining large backbones, STORM employs a multi-phase training strategy: object-centric slots are first stabilized through visual-semantic pretraining using language embeddings, then jointly adapted with a downstream manipulation policy. This staged learning prevents degenerate slot formation and preserves semantic consistency while aligning perception with task objectives. Experiments on object discovery benchmarks and simulated manipulation tasks show that STORM improves generalization to visual distractors, and control performance compared to directly using frozen foundation model features or training object-centric representations end-to-end. Our results highlight multi-phase adaptation as an efficient mechanism for transforming generic foundation model features into task-aware object-centric representations for robotic control.

Keywords: Object-centric representation · Robotics · Semantic aware.

1 Introduction

Robotic manipulation requires perceptual representations that capture fine-grained spatial structure while remaining interpretable and controllable by high-level task specifications. Recent visual foundation models such as DINOv2 [26] provide powerful dense feature representations that generalize across domains, but they do not expose explicit object-level structure. As a result, downstream policies must implicitly learn to attend to relevant entities, often leading to brittle behavior and poor generalization under visual variations [3,6].

Slot-based object-centric representation learning offers an appealing alternative. By decomposing scenes into discrete latent "slots", each representing an individual object or part, such models promote modular reasoning, interpretable structure and compositional generalization. Frameworks such as Slot-Attention [22] and its successors [9,31,33] have shown that meaningful object

representations can emerge without supervision when proper inductive biases are applied. However, these models remains **unguided**, the slot formation process is purely visual, without semantic control. As a result, the learned slots may not correspond to **task-relevant entities** [6], limiting their usefulness in action-oriented contexts such as robotics.

Recent efforts have attempted to integrate semantics into slot-based learning. Shatter & Gather [17] achieved strong alignment between slots and text post hoc through contrastive learning. CTRL-O [8] successfully demonstrated language controllability, but its training relies on several large scale visual language models (Llama2Vec [21] and CLIP [30]). While effective for object retrieval and image-generation conditioning, these approaches have yet to be adapted for robotic control scenarios, where aligning visual perception with instruction semantics is essential for manipulation. In this work, we introduce **STORM**, a lightweight slot-based task-aware module that operates on frozen DINOv2 features. Our key contributions are twofold:

Multi-phase adaptation of a visual foundation model: We introduce a two-stage learning strategy for adapting frozen visual foundation model features (DINOv2) into task-relevant, object-centric representations. The strategy first stabilizes slot formation through visual-semantic pretraining, and then aligns the same object-centric layers with downstream manipulation objectives via joint training with a control policy.

Lightweight semantic-aware object-centric representation: We propose **STORM**, a compact, stable slot-based module consisting of a small number of object-centric layers placed on top of frozen DINOv2 features. Despite its minimal architectural overhead, STORM produces semantically grounded, interpretable object representations that are directly consumable by control policies.

Overall, our results demonstrate that multi-phase strategy is an efficient ingredient for effectively transforming powerful but generic foundation model features into task-aware, object-centric representations suitable for robotic manipulation.

2 Related works

2.1 Pre-trained visual foundation models

Recent advances in visual representation learning have been driven by large-scale, self-supervised methods trained on internet-scale, unlabeled data. Many of these methods adopt Vision Transformer (ViT) architectures [10] and training objectives such as masked image modeling [13], contrastive learning [4,5,7], or hybrids that combine both paradigms [26,39]. The outcome of this line of work are highly robust pre-trained vision models (PVMs), for example DINOv2 [26], that produce rich spatially-structured features well suited for downstream perception and reasoning. At the same time, multimodal training on paired image–text corpora has produced aligned vision–language models such as CLIP [30], enabling open-vocabulary and semantic supervision for visual systems.

Most robotics pipelines today rely on such pre-trained encoders for sample-efficient policy learning [28,29,32]. However, directly using dense, high-dimensional PVM features for control can be computationally expensive and may include task-irrelevant information. In contrast, STORM produces compact, discrete slot-based latents that are both task-aware and immediately usable by downstream policies. This structured, low-dimensional output trades spatial resolution for efficiency and robustness, yielding higher throughput and reduced sensitivity to visual noise in many control settings.

2.2 Object-centric representation learning

Object-Centric Representation Learning (OCRL) formalizes the idea of decomposing scenes into a set of object-like latent “slots”, which promotes modularity and compositionality in perception. Early methods such as Slot Attention [22] demonstrated strong results on synthetic data but struggled to scale to real-world imagery. To bridge this gap, recent work has combined stronger visual backbones, for example, replacing pixel-level reconstruction targets with features from DINO [31], and has explored more expressive decoders based on Transformers or generative diffusion models [35,33,34,15,37].

A parallel strand of research seeks to ground slots semantically by leveraging external vision–language models. Approaches that use CLIP supervision or contrastive grouping encourage slots to align with human-interpretable concepts [12,17,38]. Nevertheless, slot assignments often remain underconstrained: slots can be noisy, split or merged unpredictably, and may not consistently correspond to entities that are relevant for downstream tasks. Methods like CTRL-O [8] attempt to impose language-conditioned control over slot semantics, but doing so has typically required composing multiple large models (e.g., LLM2Vec [1], CLIP), which increases system complexity and computation.

Importantly, most language-guided OCRL work to date focuses on static objectives (retrieval, segmentation, or generation). There has been limited exploration of whether text-grounded slots can serve as reliable inputs for dynamic, closed-loop control where temporal reasoning and action-affordance estimation are critical. STORM explicitly targets this gap by learning text-guided, object-centric slots and evaluating their effectiveness on robotic manipulation tasks, demonstrating that semantically aligned slots can support not only recognition but also action prediction under dynamic constraints.

2.3 Object-centric representations for robotics

Object-centric representations have recently gained significant attention in robotics as a means to improve generalization, compositionality, and data efficiency in manipulation policies [2,6,36,40]. A growing body of work leverages pre-trained segmentation and mask-based models to obtain object-level abstractions from raw visual inputs. In particular, the Segment Anything Model (SAM) [18] and its variants have been widely adopted to extract object masks that serve as intermediate representations for perception, planning, and control [28,32,40]. These

masks have been used to build object-centric state representations, to initialize object proposals for manipulation, and to enable open-vocabulary perception in conjunction with language supervision. While mask-based approaches offer strong spatial localization and benefit from powerful pre-training, they typically rely on heuristic selection, post-processing, or external prompting to identify task-relevant objects. As a result, the resulting object sets can be brittle in cluttered scenes, sensitive to occlusions, or misaligned with the objects that are most relevant for control. Moreover, segmentation masks alone provide limited semantic abstraction and often require additional processing to be integrated into downstream policies, increasing system complexity. In contrast, slot-based object-centric models learn compact, continuous representations that can encode object identity, attributes, and relations in a form that is directly consumable by control policies. However, when deployed in robotic settings, the lack of explicit control over slot formation can lead to failures under visual distraction or distributional shift [6]. This highlights a fundamental trade-off between bottom-up mask generation and learned object abstractions.

Our approach explicitly condition slot formation on task instructions and introduce a multi-phase strategy that first stabilizes semantic object discovery and then aligns object-centric representations with downstream control objectives.

3 Method

Our method, STORM (Fig. 1), extends prior object-centric learning approaches [8] with several novel design choices tailored to robotic control. The following sections detail these innovations.

3.1 Multi-phase learning for object-centric adaptation

Although frozen foundation model features provide strong visual representations, directly training object-centric layers and a control policy end-to-end often results in unstable or degenerate slot assignments, as shown in Section 4.2. To address this, we adopt a two-stage strategy that progressively introduces task supervision.

- **Stage 1: Visual–Semantic Slot Pretraining (Section 3.2):** In the first stage, the object-centric module is trained independently of the control policy. Given frozen DINOv2 [26] feature maps, STORM produces a fixed number of slots, each corresponding to a candidate object. We supervise these slots using a visual–semantic objective that aligns slot embeddings with CLIP text [30] embeddings corresponding to object-level descriptions. An additional regularization loss encourage distinct and spatially localized slot assignments. Importantly, no policy gradients are used at this stage.
- **Stage 2: Joint Slot–Policy Training (Section 3.3):** In the second stage, the pretrained object-centric module is trained alongside a downstream policy using imitation learning. The slot representations produced by the object-centric layers serve as the visual input to the policy. Crucially, the visual

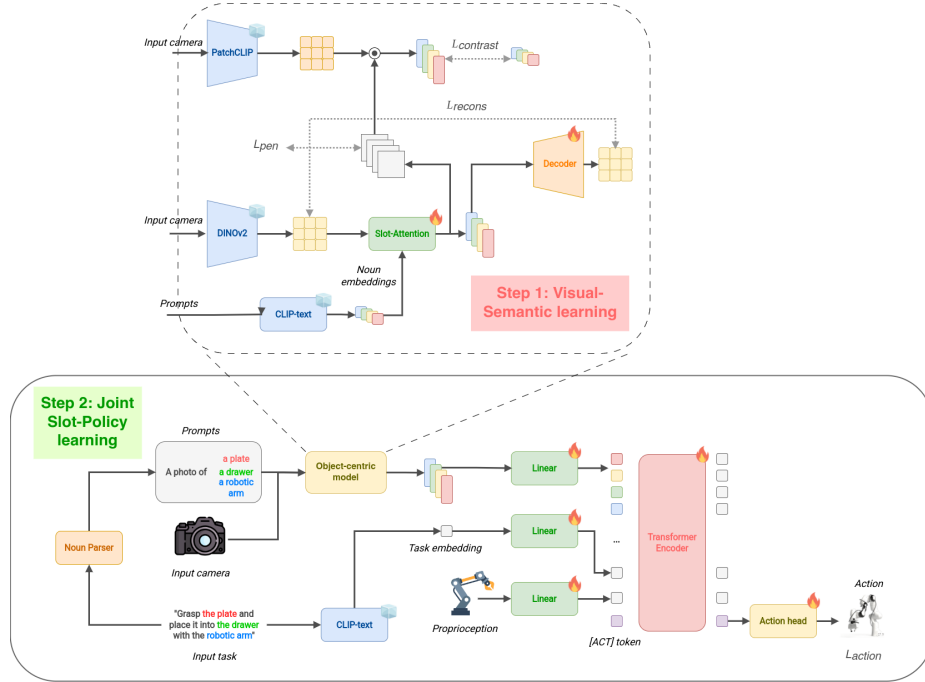


Fig. 1. Overview of STORM. STORM follows a two-stage training to produce task-aware object-centric representations for robotic control. **(Step 1) Semantic learning:** Frozen DINOv2 features are aggregated by a Slot-Attention module conditioned on noun embeddings extracted from text prompts using a frozen CLIP-text encoder. Reconstruction and contrastive losses encourage stable, semantically grounded slot formation. **(Step 2) Dynamic task alignment:** The pretrained object-centric module extracts slots from camera observations, which are combined with task embeddings, robot proprioception, and a learnable [ACT] token and processed by a Transformer decoder policy. An GMM action head predicts the next action from the [ACT] token.

module and the policy are optimized *independently*: gradients from the policy loss are not backpropagated into the visual backbone, and a gradient detachment is applied at the visual feature level. This training scheme allows the object-centric layers to preserve the semantic structure acquired during Stage 1 while adapting to task-relevant visual statistics, without destabilizing slot formation through policy-driven gradients. The resulting representations remain semantically grounded while becoming better aligned with the demands of manipulation.

This training strategy decouples object discovery from control, reducing optimization interference and leading to more robust object-centric representations. In Section 4, we empirically show that removing this multi-phase strategy significantly degrades performance, even when using identical architectures and training budgets.

3.2 Visual-Semantic learning

The first training phase focuses on properly decomposing an input image given a set of textual prompts. The framework is composed of two main parts: an object-centric decomposition and a language conditioning branch as shown in the top part of Fig. 1.

Object-centric decomposition The object-centric decomposition part follows existing works on object-centric models [31]. An input image I is encoded by a frozen DINOv2 [26] backbone B to obtain patch features $F = \{f_1, \dots, f_N\} = B(I)$. A set of slots $S = \{s_1, \dots, s_K\}$ is randomly initialized and cross-attend F with Slot-Attention [22]. Slot-Attention is a modified cross-attention with normalization over queries (slots) instead of keys (features). Finally, each slot are given to a MLP decoder in order to reconstruct the feature maps of DINOv2:

$$\mathcal{L}_{recons} = \|F - \hat{F}\| \quad (1)$$

with $\hat{F} = D(S)$, D being the MLP decoder used to reconstruct the patch features from the slots.

Language conditioning and semantic learning In order to control the generation of slots, we follow prior work [8] by initializing a part of the slots with semantic knowledge from a visual-language model. The original work uses LLM2Vec [1] to semantically initialize some slots and CLIP-text [30] to force a contrastive alignment during training. To reduce the memory and compute requirements for our robotic use case, we discard LLM2Vec and only use CLIP-text as input and training signal, going from a 7b parameters model to around 300M.

In order to align slots with textual semantics, each conditioned slot uses its corresponding mask m_k to mask-pool image patches F_{CLIP} , from a dense CLIP

visual encoder [12]. We then apply a contrastive loss between the mask-pooled visual features $F^{\text{masked}} = m_k \cdot F_{\text{CLIP}}$ and the CLIP text embeddings z_{emb} :

$$\mathcal{L}_{\text{sem}} = - \sum_{i=1}^M \log \frac{\exp(z_i^{\text{emb}} \cdot F_i^{\text{masked}} / \tau)}{\sum_{t=1}^T \exp(z_t^{\text{emb}} \cdot F_t^{\text{masked}} / \tau)}, \quad (2)$$

where $M \leq K$ denotes the number of textual prompts.

This loss encourages semantically initialized slots to bind to relevant spatial regions, but may suffer from slot collapse, where all slots attend uniformly or a single slot dominates. To mitigate this effect, we introduce an entropy-based slot usage penalty.

Let $m_k \in \mathbb{R}^{B \times K \times N}$ denote the soft assignment masks, where B is the batch size, K the number of slots, and N the number of patches. Slot collapse is quantified by aggregating slot usage (using masks weights), normalizing across slots, and computing the entropy:

$$\begin{aligned} S_{b,k} &= \sum_{n=1}^N m_{b,k,n}, & P_{b,k} &= \frac{S_{b,k}}{\sum_{j=1}^K S_{b,j} + \epsilon}, \\ \mathcal{H}_b &= -\frac{1}{\log K} \sum_{k=1}^K P_{b,k} \log(P_{b,k} + \epsilon), & \mathcal{L}_{\text{pen}} &= 1 - \frac{1}{B} \sum_{b=1}^B \mathcal{H}_b. \end{aligned} \quad (3)$$

Minimizing \mathcal{L}_{pen} encourages balanced usage of all slots and discourages degenerate solutions in which attention collapses onto a few slots.

Overall loss The model is then pre-trained by combining all the losses together:

$$\mathcal{L}_{\text{Overall}} = \mathcal{L}_{\text{recons}} + \mathcal{L}_{\text{sem}} + \mathcal{L}_{\text{pen}} \quad (4)$$

3.3 Joint Slot–Policy Training

In the second phase, we study whether semantically grounded object-centric representations improve robustness in robotic manipulation. To this end, we integrate a pretrained object-centric perception module into an imitation learning pipeline, yielding our final STORM setup.

Given a dataset of expert demonstrations $\mathcal{D} = \tau_1, \dots, \tau_n$ with trajectories $\tau_i = [(o_0, a_0), \dots, (o_T, a_T)]$, the policy π predicts actions from observations consisting of visual inputs, task instructions, and proprioceptive states.

As shown in the bottom of Fig. 1, camera observations are processed by the object-centric module to produce a fixed set of slot representations, which serve as visual tokens for the policy. Spatial features extracted from each slot’s mask are concatenated to the corresponding slot embedding. Task instructions are encoded using a frozen CLIP text encoder [30] and provided as a global task

embedding, while nouns parsed from the instruction condition the object-centric module to emphasize task-relevant entities. Proprioceptive inputs are projected as additional tokens. All tokens are processed by a Transformer decoder together with a learnable */ACT/* token. The transformer processes a history of 4 frames and predicts a sequence of 10 future actions. The action head, modeled as a Gaussian Mixture Model (GMM), maps the */ACT/* token to the next relative joint command.

The object-centric module and policy are trained jointly. To preserve semantic structure learned in Stage 1, gradients from the policy loss do not propagate into the visual part, and a feature-level gradient detachment is applied. The object-centric component is trained with a reduced learning rate and augmented with a Slot–Slot contrastive loss [24] and a single Transformer layer to encourage temporal consistency. The policy is trained using a standard imitation learning objective.

4 Experiments

We first validate our visual semantic learning on classical computer vision scenarios and compare it with existing object-centric models on object-discovery and decomposition scenarios. Then, we evaluate our task-aware multi-phase learning scheme on top of an existing VFM (DINOv2) with a simple Transformer decoder policy to learn robotic manipulation tasks. Our evaluations are performed in two different simulation benchmarks on in-domain data but also on generalization to new distractors. We finally ablate the components of our framework to understand what constitutes the success of STORM.

4.1 Object decomposition and grounding

Following prior work on object-centric representation, we first assess how effectively our visual-semantic model can discover in images.

Pre-training setup. Our visual-semantic model described in Section 3.2 is pretrained for 300k steps on the VG-COCO dataset [8] using the AdamW optimizer [23]. We use a learning rate of 4×10^{-4} with a cosine decay schedule and 10,000 warmup steps, a batch size of 64 on a single V100 GPU. We set the number of slots to 7 with a slot dimension of 256. We use the DINOv2-B/14 version.

Metrics. Object discovery performance is commonly evaluated using the *Foreground Adjusted Rand Index* (FG-ARI) [14], which quantifies segmentation accuracy and object-consistency, and *Mean Best Overlap* (mBO) [27], which measures the pixel-wise overlap between predicted and ground-truth object masks.

Object discovery. We benchmark our visual-semantic model on object-centric discovery tasks using PASCAL VOC 2012 [11] and COCO [19] datasets, both of which contain complex, multi-object scenes. These datasets are standard in the literature, allowing direct comparison with previous object-centric

methods. The goal of this evaluation is to asses how well our model separates distinct entities in an image. We follow established evaluation protocols and report results on the validation sets of both datasets.

We compare STORM against several state-of-the-art baselines: DINOSAUR [31], SPOT [16], Stable-LSD [15], Slot-Diffusion [37], and our closest baseline CTRL-O which is weakly-supervised but uses stronger semantic model as input (e.g. LLM2Vec) [8]

For all baselines, we report the results as provided in their respective papers (Table 1). STORM surpasses all unsupervised models in terms of FG-ARI and performs competitively with CTRL-O on COCO, outperforming it by 0.6 point on the mBO^i metric. While our model slightly lags in mBO compared to some methods, it clearly exceeds them in segmentation quality (FG-ARI). Note that STORM uses the original MLP decoder from DINOSAUR, which is known to produce less precise masks than transformer or diffusion decoders. Integrating such decoders could further enhance mask sharpness and overall segmentation quality.

Table 1. Object discovery performance. Metrics include mBO^i (mean Best-Overlap, instance-level), mBO^c (class-level), and FG-ARI (Foreground Adjusted Rand Index) on Pascal VOC and COCO. Bold is the best result, underline is the second best. Unsupervised (U), Weakly-Supervised (WS)

Sup.	Model	VOC			COCO		
		mBO^i	mBO^c	FG-ARI	mBO^i	mBO^c	FG-ARI
U	DINOSAUR [31]	39.5	40.9	<u>24.6</u>	27.7	30.9	40.3
	SPOT [16]	48.3	<u>55.6</u>	19.9	35.0	44.7	37.0
	Stable-LSD [15]	–	–	–	30.4	–	35.0
	Slot-Diffusion [37]	50.4	55.3	17.8	<u>31.0</u>	35.0	37.2
WS	CTRL-O [8]	–	–	–	27.2	–	47.5
	STORM (Ours)	40.6	46.5	45.8	27.8	<u>36.6</u>	<u>44.1</u>

4.2 Robotic manipulation

In our robotic manipulation experiments, we fine-tune the pre-trained object-centric layers in parallel with the policy but always keep frozen the backbone (DINOv2). The policy architecture is shared across all visual models and follows the structure detailed in Section 3.3. Joint-training is performed for 150k steps directly on the example trajectories. The visual loss is identical to that used during pre-training, but with a reduced learning rate of $1e^{-5}$ all other hyperparameters for the visual module remain unchanged. The policy is optimized using an MSE loss between the normalized predicted actions and the ground-truth actions.

Manipulation and generalization evaluations Table 2 reports the overall manipulation performance on MetaWorld [25] and LIBERO [20], evaluated both in-distribution (ID) and under new visual distractors (ND).

On MetaWorld, we observe a clear hierarchy between visual representations. The frozen DINOv2 baseline performs adequately in ID settings (73.8%) but suffers a severe degradation under visual shifts, dropping 34.2 points to 39.6% in the ND setting. Fine-tuning the backbone (DINOv2 ft.) slightly improves robustness (+4.2 points in ND) but at the cost of ID performance, suggesting a trade-off between specialization and generalization. In contrast, STORM achieves the best performance across both settings. It not only maintains strong ID accuracy (74.8%) but also substantially boosts robustness to unseen distractors, improving the ND success rate by 12.7 points over the frozen baseline.

On LIBERO, the performance gap becomes even more pronounced. While the frozen DINOv2 baseline maintains a respectable success rate of 78.9% (ID) and 70.3% (ND), fine-tuning the backbone (DINOv2 ft.) does not yield the same robustness gains observed in MetaWorld, actually resulting in slight performance drops in both settings. This suggests that standard fine-tuning may struggle with the higher visual complexity and task diversity present in the LIBERO suite. STORM, however, outperforms the best baseline by 10.7 points in ID settings and 19.3 points under new distractors. Notably, STORM exhibits almost no performance decay when transitioning from ID to ND environments on LIBERO (89.6% vs. 89.3%), whereas the baselines show a more noticeable gap. This suggests that the object-centric inductive biases in STORM allow the policy to remain focused on task-relevant features, effectively ignoring visual perturbations that typically degrade standard global representations.

Table 2. Overall evaluations Success rate (%) on **MetaWorld** and **LIBERO** benchmarks. We report performance both *In-Distribution* (ID) and under *New Distractor* (ND) conditions. Bold is the best result, underline is the second best. Relative performance to DINOv2 frozen is shown in (green) and (red).

Visual model	MetaWorld		LIBERO	
	ID \uparrow	ND \uparrow	ID \uparrow	ND \uparrow
DINOv2*	<u>73.8</u>	39.6	<u>78.9</u>	<u>70.3</u>
DINOv2 (ft.)	71.8 <small>(-2.0)</small>	<u>43.8</u> <small>(+4.2)</small>	77.5 <small>(-1.4)</small>	65.3 <small>(-5.0)</small>
STORM (Ours)	74.8 <small>(+1.0)</small>	52.3 <small>(+12.7)</small>	89.6 <small>(+10.7)</small>	89.3 <small>(+19.0)</small>

Ablation studies We conduct ablations to evaluate the effects of STORM’s key components. Specifically, we investigate: (1) the impact of the multi-phase learning, (2) the influence of different masks representations. We perform all of our ablative studies on a subset of 10 tasks from the MetaWorld [25] benchmark. We evaluate each model on in-distribution data and out-of-distribution with the

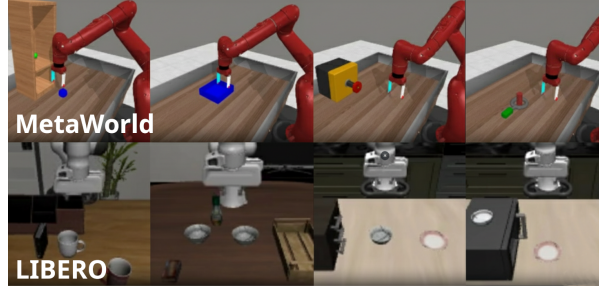


Fig. 2. Robotics environments visualization. Examples of the simulated environments used in our experiments: MetaWorld (top row) and LIBERO (bottom row).

introduction of different visual distractor objects. Results detailed in Table 3 expose that a policy relying solely on a frozen DINOv2 visual backbone already achieves strong in-distribution performance on MetaWorld. However, its generalization substantially degrades under out-of-distribution (OD) perturbations, highlighting the limitations of purely dense, non-object-centric representations when confronted with novel distractors.

Multi-phase learning Naïvely introducing object-centric slots trained from scratch on the downstream manipulation data leads to a significant performance drop in both ID and OD settings. This degradation indicates that jointly learning object decomposition and policy control from limited task-specific demonstrations is unstable and detrimental. As illustrated in the top-row of Figure 3, the resulting slot masks are noisy, poorly localized, and fail to consistently bind to task-relevant entities, which in turn negatively impacts policy learning.

Pre-training the slot-based object-centric layers and then keeping them frozen during the policy training partially alleviates this issue, yielding comparable ID performance and a notable improvement in OD generalization. Nevertheless, the best results are achieved with our proposed multi-phase training strategy (STORM), where object-centric representations are first learned independently and then carefully adapted during policy training. This decoupling stabilizes optimization and enables the slots to maintain coherent object bindings while adapting to task-specific cues, resulting in consistent improvements in both ID and OD performance.

Mask representation: In addition to learning object-centric slots, we provide the policy with explicit spatial information derived from the slot masks. Mask representations encode complementary geometric cues (object’s location, extent, and shape) that are not fully captured by appearance features alone. We evaluate three different mask encodings: `center`, which uses the mask’s center of mass; `bbox`, which encodes the bounding box coordinates; and `mask`, which directly embeds the binary mask using a shallow CNN.

Table 3. Effect of object-centric layers and multi-phase learning. Success Rate (SR) (%) on **MetaWorld**. **ID** corresponds to the standard benchmark, while **OD** corresponds to out-of-distribution evaluations. Relative performance to DINOv2 is shown in (green) and (red).

Model	Pre-train	MetaWorld (SR %)	
		ID	OD
DINOv2* [26]	–	73.8	39.6
DINOv2 (ft.)	–	71.8 (-2.0)	43.8 (+4.2)
DINOv2* + Slots scratch	✗	69.0 (-4.8)	32.5 (-7.1)
DINOv2* + Slots*	✓	72.3 (-1.5)	48.4 (+8.8)
DINOv2* + Slots tuning (STORM)	✓	74.8 (+1.0)	52.3 (+12.7)

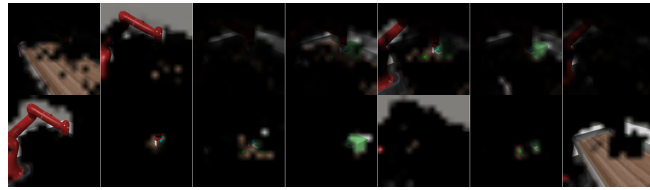


Fig. 3. Comparison of slot masks. Visualization of slot masks obtained from training from scratch (top row) versus our two-step training with adaptation (bottom row). Our setup provides much sharper masks with a focus on task-specif objects: the robot arm, the gripper, the drawer’s handle and finally the drawer body; while the training from scratch generates noisy masks with no proper focus.

Table 4 shows that incorporating mask information is crucial for strong performance. Removing mask cues leads to an important drop in success rates, confirming that spatial grounding is essential for manipulation tasks. Among the evaluated representations, the simple `center` encoding performs best on MetaWorld, outperforming more expressive alternatives, and is comparable to `mask` on MetaWorld-Gen. This suggests that a compact and stable representation of object position is sufficient, and even preferable, for policy learning. While directly encoding the full mask also yields strong results, it introduces additional complexity that does not consistently translate into higher performance. In contrast, bounding box representations appear too coarse and sensitive to noise, offering limited benefit over not using mask information at all.

5 Conclusion

We presented STORM, a slot-based, task-aware object-centric representation learning framework that integrates weak language supervision with a multi-phase training strategy for robotic manipulation. By guiding slot formation using semantic cues from task descriptions and subsequently refining these representa-

Table 4. Effect of mask representation. Success Rate (SR) (%) on **MetaWorld** and **Metaworld-Gen**. Bold is the best result, underline is the second best.

Mask repre.	MetaWorld (SR %)	Metaworld-Gen (SR %)
\emptyset	64.4	45.5
center	74.8	<u>52.3</u>
bbox	68.8	46.2
mask	<u>69.4</u>	52.8

tions through joint policy optimization, STORM achieves improved stability and performance across a range of simulated manipulation benchmarks.

Despite these gains, our approach has several limitations. Evaluations are conducted in simulation, and it remains an open question how well the learned object-centric representations transfer to real-world robotic settings. Second, STORM relies on a fixed number of slots and simple noun extraction from task descriptions, which may be insufficient for tasks involving complex relational language or a large number of objects.

Future work will explore extending STORM to real-robot platforms, incorporating more expressive language grounding mechanisms, and dynamically adapting the number and structure of slots. We also aim to investigate alternative forms of semantic supervision and more principled criteria for transitioning between training phases.

Acknowledgments .

References

1. BehnamGhader, P., Adlakha, V., Mosbach, M., Bahdanau, D., Chapados, N., Reddy, S.: Llm2vec: Large language models are secretly powerful text encoders (2024), <https://arxiv.org/abs/2404.05961>
2. Brohan, A., Brown, N., Carbajal, J., Chebotar, Y., Chen, X., Choromanski, K., Ding, T., Driess, D., Dubey, A., Finn, C., Florence, P., Fu, C., Arenas, M.G., Gopalakrishnan, K., Han, K., Hausman, K., Herzog, A., Hsu, J., Ichter, B., Irpan, A., Joshi, N., Julian, R., Kalashnikov, D., Kuang, Y., Leal, I., Lee, L., Lee, T.W.E., Levine, S., Lu, Y., Michalewski, H., Mordatch, I., Pertsch, K., Rao, K., Reymann, K., Ryoo, M., Salazar, G., Sanketi, P., Sermanet, P., Singh, J., Singh, A., Soricut, R., Tran, H., Vanhoucke, V., Vuong, Q., Wahid, A., Welker, S., Wohlhart, P., Wu, J., Xia, F., Xiao, T., Xu, P., Xu, S., Yu, T., Zitkovich, B.: Rt-2: Vision-language-action models transfer web knowledge to robotic control (2023), <https://arxiv.org/abs/2307.15818>
3. Burns, K., Witzel, Z., Hamid, J.I., Yu, T., Finn, C., Hausman, K.: What makes pre-trained visual representations successful for robust manipulation? (2023), <https://arxiv.org/abs/2312.12444>

4. Caron, M., Misra, I., Mairal, J., Goyal, P., Bojanowski, P., Joulin, A.: Unsupervised learning of visual features by contrasting cluster assignments (2021), <https://arxiv.org/abs/2006.09882>
5. Caron, M., Touvron, H., Misra, I., Jégou, H., Mairal, J., Bojanowski, P., Joulin, A.: Emerging properties in self-supervised vision transformers (2021), <https://arxiv.org/abs/2104.14294>
6. Chapin, A., Machado, B., Dellandrea, E., Chen, L.: Object-centric representations improve policy generalization in robot manipulation (2025), <https://arxiv.org/abs/2505.11563>
7. Chen, X., Xie, S., He, K.: An empirical study of training self-supervised vision transformers (2021), <https://arxiv.org/abs/2104.02057>
8. Didolkar, A., Zadaianchuk, A., Awal, R., Seitzer, M., Gavves, E., Agrawal, A.: Ctrl-o: Language-controllable object-centric visual representation learning (2025), <https://arxiv.org/abs/2503.21747>
9. Didolkar, A., Zadaianchuk, A., Goyal, A., Mozer, M., Bengio, Y., Martius, G., Seitzer, M.: Zero-shot object-centric representation learning. arXiv:2408.09162 (2024), <https://arxiv.org/abs/2408.09162>
10. Dosovitskiy, A., Beyer, L., Kolesnikov, A., Weissenborn, D., Zhai, X., Unterthiner, T., Dehghani, M., Minderer, M., Heigold, G., Gelly, S., Uszkoreit, J., Houlsby, N.: An image is worth 16x16 words: Transformers for image recognition at scale (2021), <https://arxiv.org/abs/2010.11929>
11. Everingham, M., Gool, L.V., Williams, C.K.I., Winn, J., Zisserman, A.: The pascal visual object classes (voc) challenge. International Journal of Computer Vision **88**(2), 303–338 (2010). <https://doi.org/10.1007/s11263-009-0275-4>
12. Fan, K., Bai, Z., Xiao, T., Zietlow, D., Horn, M., Zhao, Z., Simon-Gabriel, C.J., Shou, M.Z., Locatello, F., Schiele, B., Brox, T., Zhang, Z., Fu, Y., He, T.: Unsupervised open-vocabulary object localization in videos (2024), <https://arxiv.org/abs/2309.09858>
13. He, K., Chen, X., Xie, S., Li, Y., Dollár, P., Girshick, R.: Masked autoencoders are scalable vision learners (2021), <https://arxiv.org/abs/2111.06377>
14. Hubert, L., Arabie, P.: Comparing partitions. Journal of Classification **2**(1), 193–218 (1985). <https://doi.org/10.1007/BF01908075>
15. Jiang, J., Deng, F., Singh, G., Ahn, S.: Object-centric slot diffusion (2023), <https://arxiv.org/abs/2303.10834>
16. Kakogeorgiou, I., Gidaris, S., Karantzalos, K., Komodakis, N.: Spot: Self-training with patch-order permutation for object-centric learning with autoregressive transformers (2024), <https://arxiv.org/abs/2312.00648>
17. Kim, D., Kim, N., Lan, C., Kwak, S.: Shatter and gather: Learning referring image segmentation with text supervision (2023), <https://arxiv.org/abs/2308.15512>
18. Kirillov, A., Mintun, E., Ravi, N., Mao, H., Rolland, C., Gustafson, L., Xiao, T., Whitehead, S., Berg, A.C., Lo, W.Y., Dollár, P., Girshick, R.: Segment anything (2023), <https://arxiv.org/abs/2304.02643>
19. Lin, T.Y., Maire, M., Belongie, S., Bourdev, L., Girshick, R., Hays, J., Perona, P., Ramanan, D., Zitnick, C.L., Dollár, P.: Microsoft coco: Common objects in context (2015), <https://arxiv.org/abs/1405.0312>
20. Liu, B., Zhu, Y., Gao, C., Feng, Y., Liu, Q., Zhu, Y., Stone, P.: Libero: Benchmarking knowledge transfer for lifelong robot learning. arXiv preprint arXiv:2306.03310 (2023)
21. Liu, Z., Li, C., Xiao, S., Shao, Y., Lian, D.: Llama2vec: Unsupervised adaptation of large language models for dense retrieval (2025), <https://arxiv.org/abs/2312.15503>

22. Locatello, F., Weissenborn, D., Unterthiner, T., Mahendran, A., Heigold, G., Uszkoreit, J., Dosovitskiy, A., Kipf, T.: Object-centric learning with slot attention (2020), <https://arxiv.org/abs/2006.15055>
23. Loshchilov, I., Hutter, F.: Decoupled weight decay regularization (2019), <https://arxiv.org/abs/1711.05101>
24. Manasyan, A., Seitzer, M., Radovic, F., Martius, G., Zadaianchuk, A.: Temporally consistent object-centric learning by contrasting slots (2025), <https://arxiv.org/abs/2412.14295>
25. McLean, R., Chatzaroulas, E., McCutcheon, L., Röder, F., Yu, T., He, Z., Zentner, K.R., Julian, R., Terry, J.K., Woungang, I., Farsad, N., Castro, P.S.: Meta-world+: An improved, standardized, rl benchmark (2025), <https://arxiv.org/abs/2505.11289>
26. Oquab, M., Dariseti, T., Moutakanni, T., Vo, H., Szafraniec, M., Khalidov, V., Fernandez, P., Haziza, D., Massa, F., El-Nouby, A., Assran, M., Ballas, N., Galuba, W., Howes, R., Huang, P.Y., Li, S.W., Misra, I., Rabbat, M., Sharma, V., Synnaeve, G., Xu, H., Jegou, H., Mairal, J., Labatut, P., Joulin, A., Bojanowski, P.: Dinov2: Learning robust visual features without supervision (2024), <https://arxiv.org/abs/2304.07193>
27. Pont-Tuset, J., Arbelaez, P., T.Barron, J., Marques, F., Malik, J.: Multiscale combinatorial grouping for image segmentation and object proposal generation. *IEEE Transactions on Pattern Analysis and Machine Intelligence* **39**(1), 128–140 (Jan 2017). <https://doi.org/10.1109/tpami.2016.2537320>, <http://dx.doi.org/10.1109/TPAMI.2016.2537320>
28. Qian, J., Li, Y., Bucher, B., Jayaraman, D.: Task-oriented hierarchical object decomposition for visuomotor control (2024), <https://arxiv.org/abs/2411.01284>
29. Qian, J., Panagopoulos, A., Jayaraman, D.: Recasting generic pretrained vision transformers as object-centric scene encoders for manipulation policies (2024), <https://arxiv.org/abs/2405.15916>
30. Radford, A., Kim, J.W., Hallacy, C., Ramesh, A., Goh, G., Agarwal, S., Sastry, G., Askell, A., Mishkin, P., Clark, J., Krueger, G., Sutskever, I.: Learning transferable visual models from natural language supervision (2021), <https://arxiv.org/abs/2103.00020>
31. Seitzer, M., Horn, M., Zadaianchuk, A., Zietlow, D., Xiao, T., Simon-Gabriel, C.J., He, T., Zhang, Z., Schölkopf, B., Brox, T., Locatello, F.: Bridging the gap to real-world object-centric learning (2023), <https://arxiv.org/abs/2209.14860>
32. Shi, J., Qian, J., Ma, Y.J., Jayaraman, D.: Composing pre-trained object-centric representations for robotics from "what" and "where" foundation models (2024), <https://arxiv.org/abs/2404.13474>
33. Singh, G., Deng, F., Ahn, S.: Illiterate dall-e learns to compose (2022), <https://arxiv.org/abs/2110.11405>
34. Singh, G., Wu, Y.F., Ahn, S.: Simple unsupervised object-centric learning for complex and naturalistic videos (2022), <https://arxiv.org/abs/2205.14065>
35. Singh, K., Schaub-Meyer, S., Roth, S.: Glass: Guided latent slot diffusion for object-centric learning (2025), <https://arxiv.org/abs/2407.17929>
36. Wen, X., Zhao, B., Chen, Y., Pang, J., Qi, X.: A data-centric revisit of pre-trained vision models for robot learning (2025), <https://arxiv.org/abs/2503.06960>
37. Wu, Z., Hu, J., Lu, W., Gilitschenski, I., Garg, A.: Slotdiffusion: Object-centric generative modeling with diffusion models (2023), <https://arxiv.org/abs/2305.11281>

38. Xu, J., Mello, S.D., Liu, S., Byeon, W., Breuel, T., Kautz, J., Wang, X.: Groupvit: Semantic segmentation emerges from text supervision (2022), <https://arxiv.org/abs/2202.11094>
39. Zhou, J., Wei, C., Wang, H., Shen, W., Xie, C., Yuille, A., Kong, T.: ibot: Image bert pre-training with online tokenizer (2022), <https://arxiv.org/abs/2111.07832>
40. Zhu, Y., Jiang, Z., Stone, P., Zhu, Y.: Learning generalizable manipulation policies with object-centric 3d representations (2023), <https://arxiv.org/abs/2310.14386>